Complex Systems **3** (1989) 317–330

Lattice Boltzmann Equation for Laminar Boundary flow

Paul Lavallée
Physics Department, Université du Québec à Montréal, CP 8888, Montréal H3C 3P8, Canada

Jean Pierre Boon
Alain Noullez
Faculté des Sciences, Université Libre de Bruxelles, CP 231, Bruxelles, Belgique B1050, France

Abstract. A simple method based on the lattice Boltzmann equation is presented for the evaluation of the velocity profile of fluid flows near walls or in the vicinity of the interface between two fluids. The method is applied to fluid flow near a wall, to channel flow, and to the transition zone between two fluids flowing parallel to each other in opposite directions. The results show good agreement with microdynamical lattice gas simulations and with classical fluid dynamics.

1. The lattice boundary layer problem

Since the pioneering work by Hardy, Pomeau, and de Pazzis in 1973 [1,2], Wolfram in 1983 [3], and mostly since the recent introduction of the hexagonal lattice gas by Frisch, Hasslacher, and Pomeau [4], lattice gas methods have evolved both in efficiency and complexity (an extensive introduction to the subject can be found in [5]). The theoretical and computational development of the field has been so extensive in the last couple of years that it has given rise to applications in various areas of physics [6].

Lattice gases share common operational features with cellular automata and so are most easily implemented on parallel machines, in particular for fluid dynamical problems at large Reynolds numbers [7] which require high computational performances. On the other hand, there exists a variety of operationally simple problems of valuable physical interest that can be solved with modest computational means for which small computers provide sufficient power. For the class of problems considered here, the lattice gas flow description can be reduced to a "one-dimensional" formulation; therefore such problems can be solved with low power computational techniques.

The formation and growth of boundary layers is of crucial importance in fluid dynamical flows, in particular as their occurrence triggers the development of turbulence at high Reynolds numbers. For viscous flow (at low Reynolds number), boundary layer problems can be solved within the limits of reasonable approximations. Such problems so appear as an interesting test for the validity of the lattice gas method and their solutions are a prerequisite to the understanding of more complex flows and of the three-dimensionalization in the transition to turbulence. The purpose of the present work is to show that laminar boundary flow can be treated efficiently, that is, simply and economically, by the lattice gas method.

The basic idea is the following: consider that a lattice gas, initially in homogeneous unidirectional motion, is suddenly put in contact with a wall. All lattice gas nodes in any layer parallel to the flow direction have the same particle distribution and, the system being translationally invariant, it suffices to perform one-dimensional computation to evaluate the velocity profile. The wall effects on the flow velocity are propagated by the particles at the microscopic "thermal velocity," whereas the flow profile modifications propagate via particle interactions, i.e., at much lower speed. Interactions with the wall will first be felt on the first layer of the gas (i.e., the layer adjacent to the wall); at the next time step, they will be felt on the first and second layers, and progressively the successive lattice layers will be interactively involved. More precisely, we consider a gas (density d) flowing parallel to a wall with free flow velocity Uo. Momentum is first exchanged between the wall and the first layer: the flow is slowed down in that layer due to velocity reversal of the particles colliding with the wall. The first layer will come to a state of local equilibrium acquiring velocity U parallel to the wall with $U < Uo$. All layers beyond the first one remain at the free flow velocity Uo.

During the second time step, the transport of the particles from the first layer will affect the second layer of the gas: particles in the second layer are now slowed down due to the lower velocity in the first layer. The new equilibrium populations in the first and second layers are computed. The third step in the process will affect the third layer of the gas; however, the fresh values of the second layer computed from the second time step will exert an influence on the first layer so that equilibrium values for the first two layers must be updated before that of the third be evaluated.

At each time step of the process, the new equilibrium values of each underlying layer are updated from the fresh values obtained for the upper and lower adjacent layers at the previous step and the next upper layer is included in the computation. At any given time, all the layers that have reached equilibrium and have a velocity value $U \leq 0.99Uo$ are considered to belong to the boundary layer. Because of the discreteness of the lattice, the exact value of the boundary layer thickness δ must be evaluated (in general) by interpolation. The boundary layer thickness growth is much slower than the increase in the number of layers: the boundary layer thickness grows as the square root of the number of time steps [8], whereas the number of layers is equal to the number of time steps. All the layers that have not

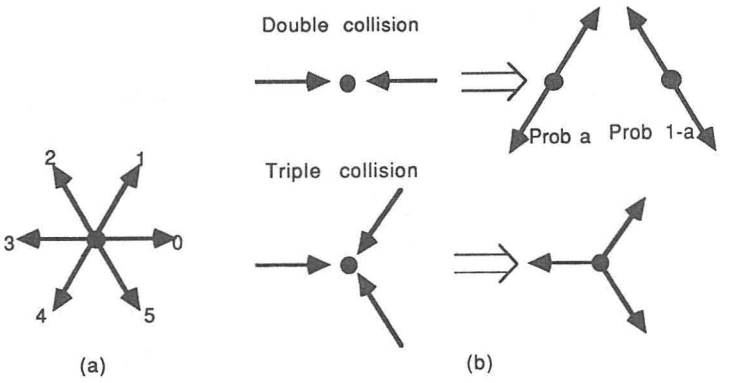

Figure 1: (a) Indices for velocity orientations on lattice nodes; (b) collision rules.

yet been included in the calculation are assumed to be at equilibrium with velocity Uo.

The physical situation described by the calculation outlined above can be viewed in the following way: a gas at rest in contact with a wall ($t < 0$) is suddenly made to move instantaneously (at $t = 0$) with velocity Uo in the positive x direction (it is assumed that the gas reaches stationary velocity Uo instantaneously). Each "column" of particles behaves like its neighbors and the boundary layer grows in a similar way for all columns. At the next time step, the boundary layer thickness δ will have grown by an equal amount for all columns and the number of time steps elapsed can be interpreted either as time (distance from the wall) or space (distance along the wall). Hence we obtain "two-dimensional" information from a "one-dimensional" formulation, with restriction to situations where the flow is parallel to the boundary (extension to plane laminar two-fluid flow is straightforward).

2. The lattice gas model

We use the FHP hexagonal lattice gas with standard collision rules [9]: only head-on and triple collisions (shown in figure 1b) lead to momentum transfer; all other collisions are "transparent." No rest particles are included here for simplicity. (We also performed computations with a model including rest particles and obtained essentially the same results).

With the indices as given in figure 1a, the microdynamical equations for the occupancy states n_i (which can be only 0 or 1 due to the lattice gas exclusion principle [9]) are

$$n_i(t+1, \boldsymbol{r} + \boldsymbol{c}_i) = n_i(t, \boldsymbol{r}) + \Delta_i(n); \quad i = 0, 1, \ldots, 5 \tag{2.1}$$

where $n_i(t, \boldsymbol{r})$ is the propagation term and $\Delta_i(n)$ denotes the collision term.

$$\Delta_i(n) = \Delta_i^{(2)}(n) + \Delta_i^{(3)}(n)$$

$$\begin{aligned}
\Delta_i^{(2)}(n) &= a n_{i+1}(t,\boldsymbol{r}) n_{i+4}(t,\boldsymbol{r}) \underline{n}_i(t,\boldsymbol{r}) \underline{n}_{i+2}(t,\boldsymbol{r}) \underline{n}_{i+3}(t,\boldsymbol{r}) \underline{n}_{i+5}(t,\boldsymbol{r}) \\
&+ (1-a) n_{i+2}(t,\boldsymbol{r}) n_{i+5}(t,\boldsymbol{r}) \underline{n}_i(t,\boldsymbol{r}) \underline{n}_{i+1}(t,\boldsymbol{r}) \\
&\quad \underline{n}_{i+3}(t,\boldsymbol{r}) \underline{n}_{i+4}(t,\boldsymbol{r}) \\
&- n_i(t,\boldsymbol{r}) n_{i+3}(t,\boldsymbol{r}) \underline{n}_{i+1}(t,\boldsymbol{r}) \underline{n}_{i+2}(t,\boldsymbol{r}) \\
&\quad \underline{n}_{i+4}(t,\boldsymbol{r}) \underline{n}_{i+5}(t,\boldsymbol{r}) \qquad (2.2)
\end{aligned}$$

$$\begin{aligned}
\Delta_i^{(3)}(n) &= n_{i+1}(t,\boldsymbol{r}) n_{i+3}(t,\boldsymbol{r}) n_{i+5}(t,\boldsymbol{r}) \underline{n}_i(t,\boldsymbol{r}) \underline{n}_{i+2}(t,\boldsymbol{r}) \underline{n}_{i+4}(t,\boldsymbol{r}) \\
&- n_i(t,\boldsymbol{r}) n_{i+2}(t,\boldsymbol{r}) n_{i+4}(t,\boldsymbol{r}) \underline{n}_{i+1}(t,\boldsymbol{r}) \underline{n}_{i+3}(t,\boldsymbol{r}) \underline{n}_{i+5}(t,\boldsymbol{r})
\end{aligned}$$

where $\Delta_i^{(2)}(n)$ and $\Delta_i^{(3)}(n)$ are the contributions from binary collisions and from triple collisions respectively, and a is defined in figure 1b. $\Delta_i(n)$ can take the values -1, 0, or $+1$. Equations (2.1) and (2.2) are the microdynamical equations for the hexagonal lattice gas model (without rest particles). The microdynamical equations set the local rules which are used for lattice gas simulations.

The passage from the deterministic description to a probabilistic one is made via the Liouville equation which expresses the probability of finding the system in a given state from the knowledge of its state at an earlier time. Then, we can define averaged quantities as

$$N_i(t,r) = < n_i(t,\boldsymbol{r}) >$$

whose evolution is governed by the equation

$$\begin{aligned}
N_i(t+1, r+\boldsymbol{c}_i) &= N_i(t,\boldsymbol{r}) \\
&+ < a n_{i+1}(t,\boldsymbol{r}) n_{i+4}(t,\boldsymbol{r}) \underline{n}_i(t,\boldsymbol{r}) \\
&\quad n_{i+2}(t,\boldsymbol{r}) \underline{n}_{i+3}(t,\boldsymbol{r}) \underline{n}_{i+5}(t,\boldsymbol{r}) > \\
&+ < (1-a) n_{i+2}(t,\boldsymbol{r}) n_{i+5}(t,\boldsymbol{r}) \underline{n}_i(t,\boldsymbol{r}) \\
&\quad \underline{n}_{i+1}(t,\boldsymbol{r}) \underline{n}_{i+3}(t,\boldsymbol{r}) \underline{n}_{i+4}(t,\boldsymbol{r}) > \\
&- < n_i(t,\boldsymbol{r}) n_{i+3}(t,\boldsymbol{r}) \underline{n}_{i+1}(t,\boldsymbol{r}) \\
&\quad \underline{n}_{i+2}(t,\boldsymbol{r}) \underline{n}_{i+4}(t,\boldsymbol{r}) \underline{n}_{i+5}(t,\boldsymbol{r}) > \\
&+ < n_{i+1}(t,\boldsymbol{r}) n_{i+3}(t,\boldsymbol{r}) n_{i+5}(t,\boldsymbol{r}) \\
&\quad \underline{n}_i(t,\boldsymbol{r}) \underline{n}_{i+2}(t,\boldsymbol{r}) \underline{n}_{i+4}(t,\boldsymbol{r}) > \\
&- < n_i(t,\boldsymbol{r}) n_{i+2}(t,\boldsymbol{r}) n_{i+4}(t,\boldsymbol{r}) \\
&\quad \underline{n}_{i+1}(t,\boldsymbol{r}) \underline{n}_{i+3}(t,\boldsymbol{r}) \underline{n}_{i+5}(t,\boldsymbol{r}) > \qquad (2.3)
\end{aligned}$$

With the Boltzmann approximation, i.e., assuming that there is no correlation between particles prior to collision, which amounts to setting:

$$< n_i n_j > = < n_i >< n_j > = N_i N_j, \qquad (2.4)$$

one obtains the "lattice gas Boltzmann equation"

$$N_i(t+1, \boldsymbol{r}+\boldsymbol{c}_i) = N_i(t, \boldsymbol{r}) + \Delta_i(n) \tag{2.5}$$

$$\begin{aligned}
\Delta_i(n) \;=\; & +0.5 N_{i+1}(t,\boldsymbol{r}) N_{i+4}(t,\boldsymbol{r}) \underline{N}_i(t,\boldsymbol{r}) \\
& \underline{N}_{i+2}(t,\boldsymbol{r}) \underline{N}_{i+3}(t,\boldsymbol{r}) \underline{N}_{i+5}(t,\boldsymbol{r}) \\
& + \; 0.5 N_{i+2}(t,\boldsymbol{r}) N_{i+5}(t,\boldsymbol{r}) \underline{N}_i(t,\boldsymbol{r}) \\
& \underline{N}_{i+1}(t,\boldsymbol{r}) \underline{N}_{i+3}(t,\boldsymbol{r}) \underline{N}_{i+4}(t,\boldsymbol{r}) \\
& - \; N_i(t,\boldsymbol{r}) N_{i+3}(t,\boldsymbol{r}) \underline{N}_{i+1}(t,\boldsymbol{r}) \\
& \underline{N}_{i+2}(t,\boldsymbol{r}) \underline{N}_{i+4}(t,\boldsymbol{r}) \underline{N}_{i+5}(t,\boldsymbol{r}) \\
& + \; N_{i+1}(t,\boldsymbol{r}) N_{i+3}(t,\boldsymbol{r}) N_{i+5}(t,\boldsymbol{r}) \\
& \underline{N}_i(t,\boldsymbol{r}) \underline{N}_{i+2}(t,\boldsymbol{r}) \underline{N}_{i+4}(t,\boldsymbol{r}) \\
& - \; N_i(t,\boldsymbol{r}) N_{i+2}(t,\boldsymbol{r}) N_{i+4}(t,\boldsymbol{r}) \\
& \underline{N}_{i+1}(t,\boldsymbol{r}) \underline{N}_{i+3}(t,\boldsymbol{r}) \underline{N}_{i+5}(t,\boldsymbol{r})
\end{aligned} \tag{2.6}$$

where we have set $a = 0.5$ (equal probabilities for binary collision output states).

Solving the lattice Boltzmann equation offers an alternative to microdynamical simulations; however the variables are then continuous rather than Boolean. From (2.5) the ensemble averaged hydrodynamic quantities, e.g., the density and the velocity field are obtained.

$$\rho = \sum N_i; \quad U = 1/\rho \sum (N_i \boldsymbol{c}_i) \tag{2.7}$$

3. Interaction with a solid boundary

We next consider the interaction mechanism of the gas with the wall. Particles can undergo pure specular reflections, "bounce-back" reflections (figure 2) or any combination of these. Pure specular reflections meet the condition of a perfectly slippery boundary and should not affect the velocity profile of the flow (this feature can be used as a test to check whether the model is performing correctly). Pure bounce-back reflections yield zero flow velocity along the wall, which corresponds to no-slip condition. The model

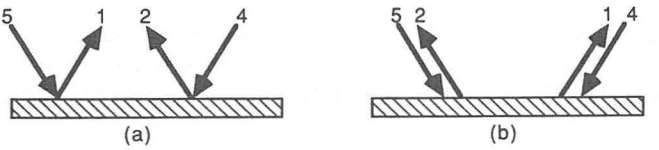

Figure 2: (a) Specular reflection; (b) bounce-back reflection.

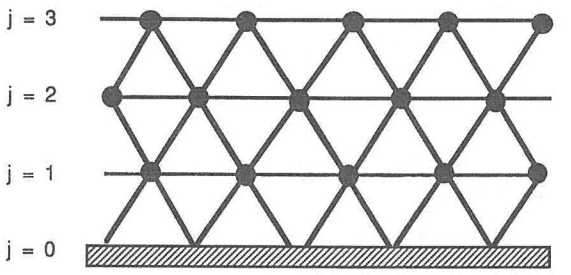

Figure 3: Configuration of the lattice near the wall.

can be implemented so as to handle either type of reflection or a combination of both in any proportion.

Knudsen's experimental results suggest that, in a real system, the gas molecules impinging on a wall at a constant angle of incidence are reflected back in randomly distributed directions [10]. This corresponds to a combination of equally weighted specular and bounce-back reflections in a lattice gas (that is a bounce-back reflection coefficient $r = 0.5$, with $r = 1$ for pure bounce-back reflections). However, the interaction mechanism in a lattice gas differs from that of a real gas in that all interactions on the lattice are synchronized and particles can only be located at "quantized" distances from the wall. This should be taken into account if the model is to match actual situations.

The wall is denoted as row number zero ($j = 0$) in the model configuration (figure 3). Since particle velocities can be oriented in only two directions on row number zero (particles are not allowed to move tangentially on the wall), no equilibrium state is computed for this row. A particle leaving row number one at time t along direction 4(5) will necessarily return to row one at time $t + 2$ as a particle in direction 2(1) after specular reflection or direction 1(2) after bounce-back reflection. The computation proceeds as explained in section 1, the wall acting as a "reflector" for particles.

4. Flow parallel to a solid boundary

We first examine fluid flow parallel to a flat wall. The translational invariance and the orthogonality of the flow direction of the model eliminate the advection term $\boldsymbol{U} \cdot \boldsymbol{\nabla U}$ in the Navier-Stokes equation which reduces to:

$$\frac{\partial u}{\partial t} = \nu \frac{\partial^2 u}{\partial y^2}$$

where u is the x component of $\boldsymbol{U}$ and ν is the kinematic viscosity. The solution to this equation reads [8]:

$$U = Uoerf\{y/(4\nu t)^{1/2}\} \tag{4.1}$$

The results of the lattice Boltzmann computation are given in figure 4 for the first few time steps of the boundary layer growth and its later evolution. When the boundary layer becomes sufficiently thick (approximately after five time steps), the characteristic velocity profile of laminar boundary flow emerges clearly. The boundary layer thickness is seen to broaden as time progresses. These results are confirmed by our lattice gas simulations. In figure 5, we compare the simulation velocity profile with the theoretical error function profile (the Blasius profile [11] is given as a reference).

Theory predicts that the boundary layer thickness grows as the square root of the distance from the leading edge of the wall. Figure 6 shows that the results of the lattice gas simulation are in excellent agreement with theory (as soon as the number of layers in the boundary exceeds three). Note that the results obtained for the error function profile and for the boundary layer growth are also in good agreement with lattice gas simulations performed with the microdynamical equations [12].

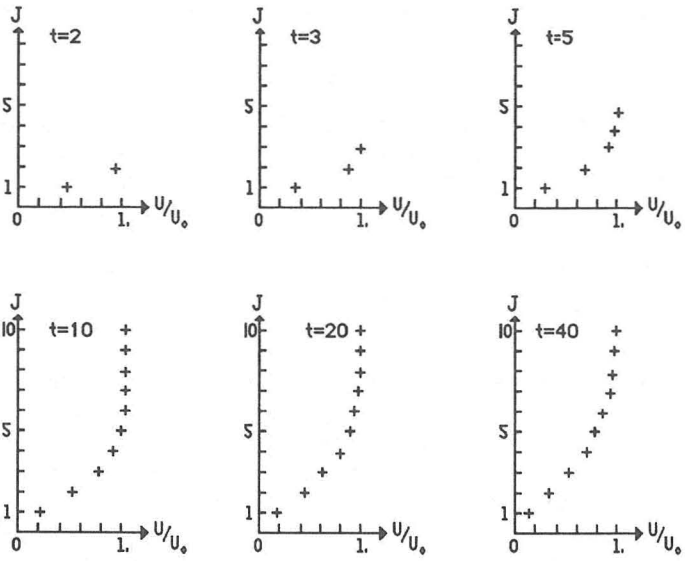

Figure 4: Velocity profile obtained from lattice Boltzmann computation of flow parallel to a horizontal flat wall. Gas density $d = 0.233$; free-flow velocity $Uo = 0.35$; j denotes the lattice row number (wall at $j = 0$); time t is given in lattice time step units; bounce-back reflection coefficient $r = 1$.

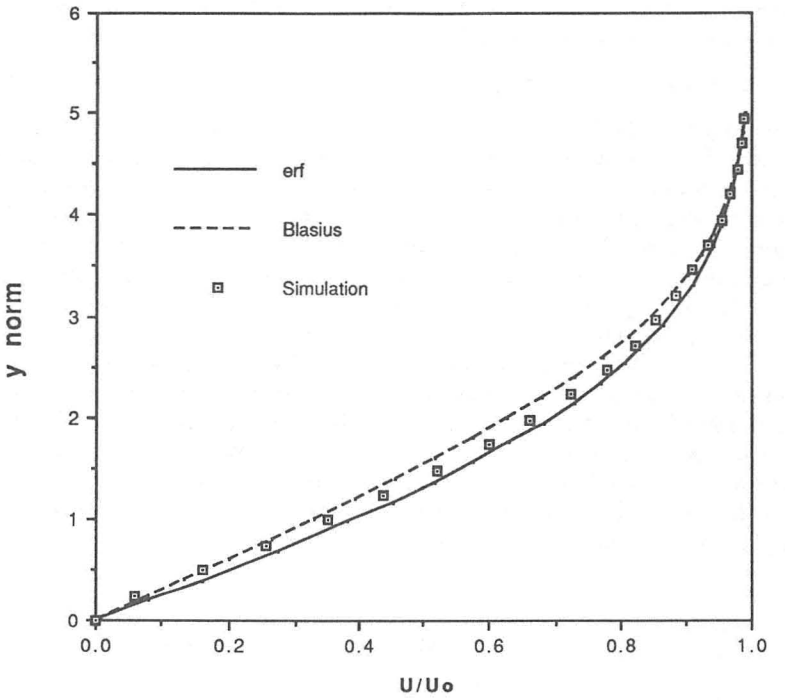

Figure 5: Theoretical error function and Blasius profiles and lattice gas simulation data after 150 time steps (particle density $d = 0.1833$, free-flow velocity $Uo = 2.72$, bounce-back reflection coefficient $r = 1$). y norm is the normalized space coordinate measuring the distance from the wall. y norm $= 4.99j/jo$ where jo is the interpolated row index value corresponding to $U = 0.99Uo$. The factors 4.99 and 0.99 are standard in boundary layer theory [11].

We next examine the effect of the bounce-back reflection coefficient r. We observe that deviations from the theoretical profile increase as r decreases (figure 7). As soon as specular reflections are present, the velocity on the wall becomes nonzero. This velocity component can be evaluated from the values of the velocity components toward the wall on layer 1. The experiments conducted by Knudsen show that a ratio $r = 0.5$ would be appropriate [10]. This apparent discrepancy can be explained by the fact that in lattice gases, no particle can be closer to the wall than one interlayer distance, whereas in real gases, the average distance of molecules from the wall is of the order of the mean-free path: unless the gas is extremely rarefied, the velocity on the wall is vanishingly small. However, if a lattice gas simulation with a reflection coefficient $r = 0.5$ is run for a sufficiently long time, velocity on the wall will get arbitrarily close to zero. On the other hand, pure specular reflection

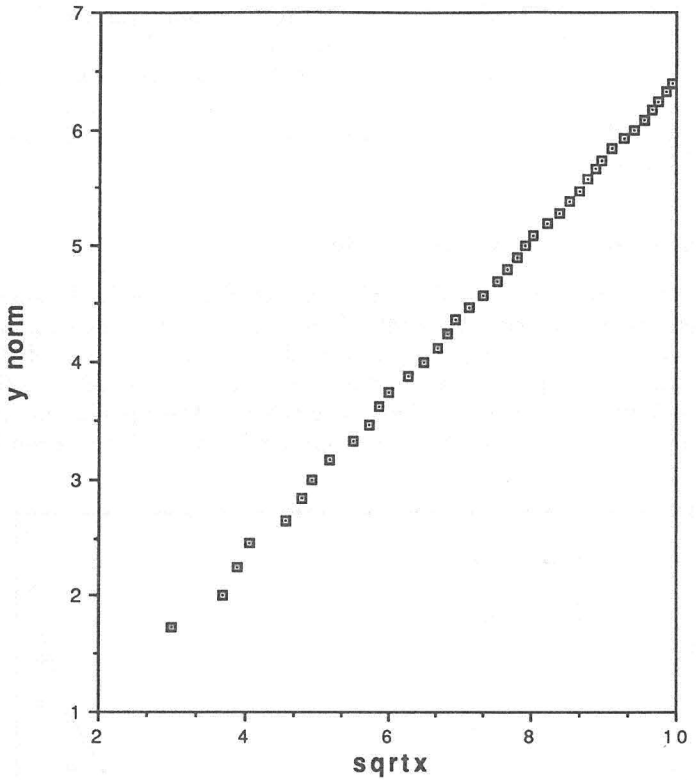

Figure 6: Boundary layer growth with distance (up to 41 distance units). Same conditions as given in caption of figure 4. y norm is defined in caption of figure 5. The distance from the leading edge is tU^*. Since the boundary layer thickness is defined at $U^* = 0.99Uo$, we define x by converting directly t into distance (ignoring the constant factor U^*).

conditions produce no boundary layer whatsoever, as expected (perfect slip on the wall).

5. Channel flow

We consider two walls separated by an integer number of layers and impose the appropriate reflection rules on these walls. The limitations of the method are obvious in channel flow simulation. In the flow near a wall as investigated in section 4, the gas with a velocity Uo away from the boundary layer acts as the driving force for the whole fluid. In channel flow, as soon as the two boundary layers meet, this driving force is no longer present, and friction

progressively brings the fluid to rest. Therefore, appropriate scaling must be introduced to display our computational results as Poiseuille flow. The comparison with theory is shown in figure 8. We also obtain good agreement with channel flow simulations from the microdynamical equations [12–14] (Note that [13] shows channel flows that have not yet fully developed to Poiseuille flows.)

6. Transition zone in two-fluid flow

We consider two-fluid flow and examine the velocity profile in the transition zone between two gases with identical physical properties flowing parallel to each other. The separation layer is labeled with index zero and the net velocity component parallel to the flow direction at $j = 0$ is $U = 0$ (in the reference frame of the mean of the two velocities). The equilibrium state at time t for each layer (j) is computed from the Ni values for adjacent layers

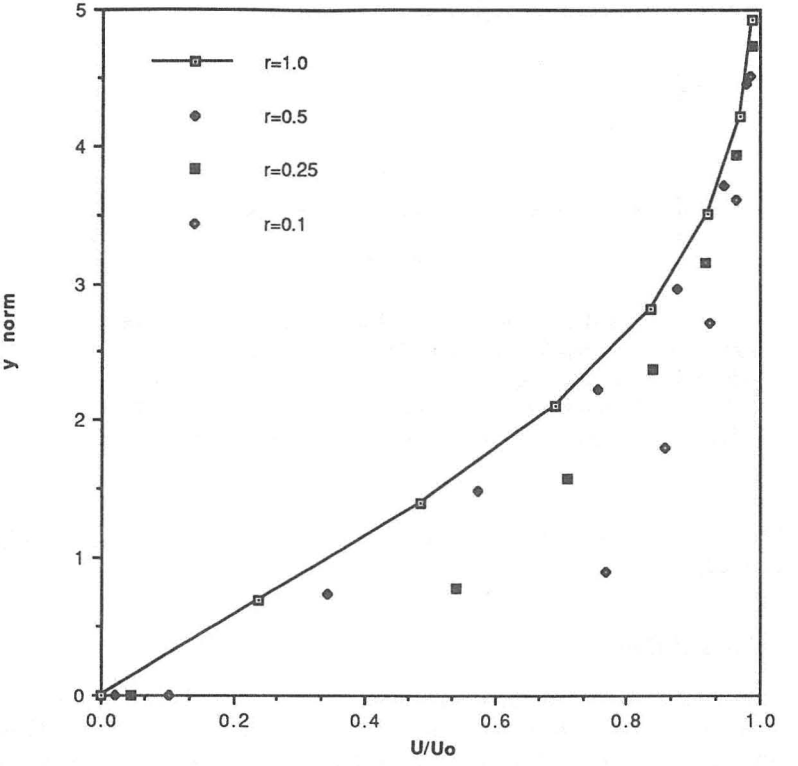

Figure 7: Velocity profiles for various bounce-back reflection ratios. (Gas density: $d = 0.233$; free-flow velocity: $Uo = 0.500$). The data shown were obtained after 20 time steps.

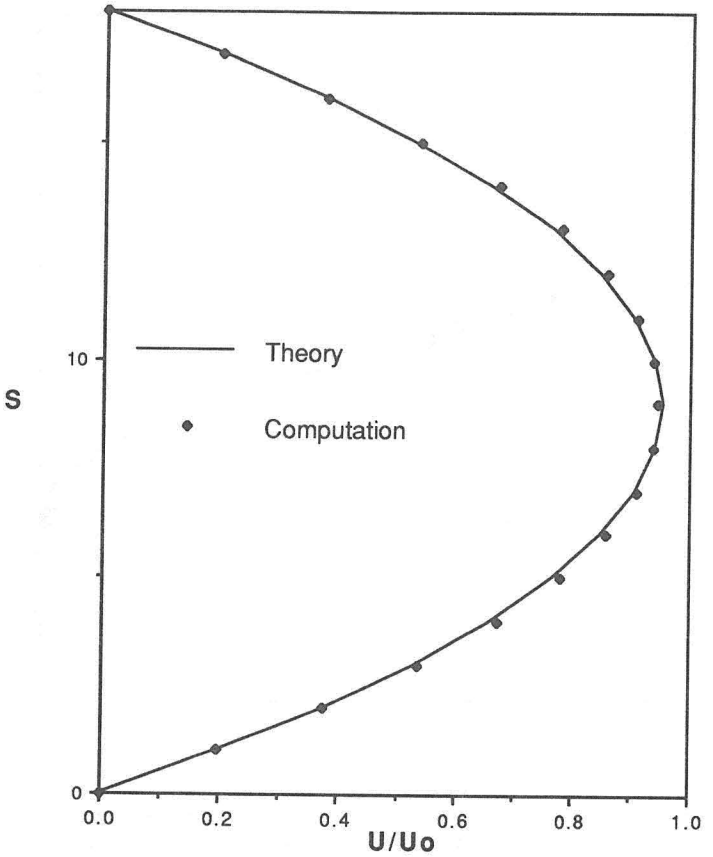

Figure 8: Comparison of lattice Boltzmann computation of channel flow with scaled theoretical Poiseuille flow (S is the transverse distance in the channel measured in lattice units; channel width is 18 lattice units; particle density $d = 0.267$; free-flow velocity $Uo = 0.312$; reflection coefficient $r = 0.5$). The profile is shown after 47 time steps.

$j+1$ and $j-1$, and layer j itself, evaluated at time $(t-1)$. From classical hydrodynamics, the solution to this problem, for flows in opposite directions, reads as for the flow parallel to a wall [8]:

$$U = Uoerf\{y/(4\nu t)^{1/2}\} \tag{6.1}$$

where $2Uo$ is now the difference between the two velocities and y is the continuous variable corresponding to j (with $y = 0$ corresponding to $j = 0$); ν is the kinematic velocity. Here the kinematic viscosity ν is computed from

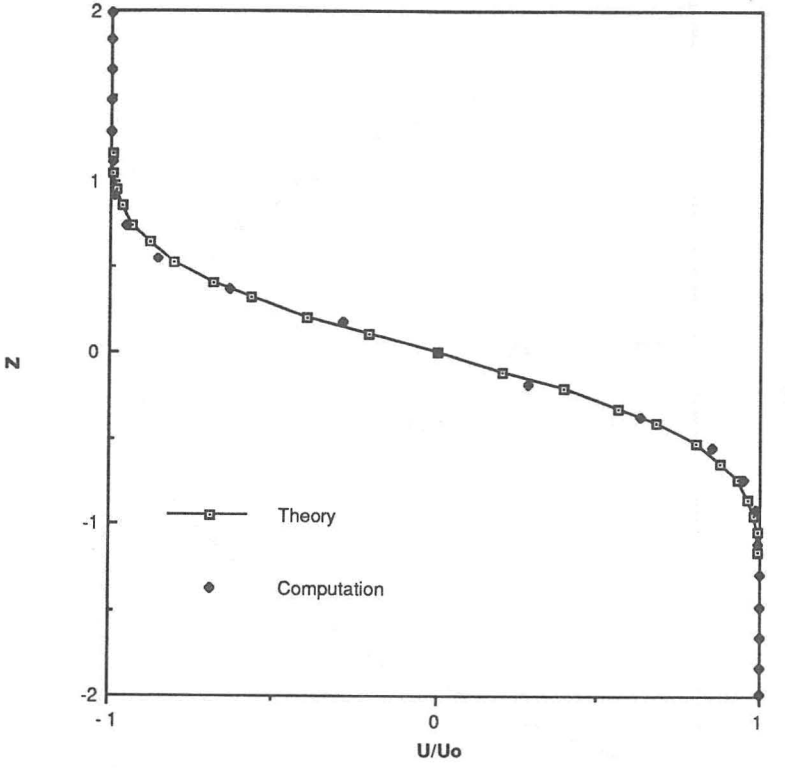

Figure 9: Transition zone between two anti-parallel flows: comparison between theory (6.1) and Boltzmann computation. Z is the normalized distance variable $Z = y\sqrt{4\nu t}$. Upper gas flow velocity $U1 = -0.1$, lower gas flow velocity $U2 = +0.1$. Density for both gases is $d = 0.25$. The profile shown was obtained after 11 time steps of computation.

the actual collision rules of the model [9]. The Boltzmann computation[1] yields excellent agreement with the theoretical expression as illustrated in figure 9; recent microdynamical simulations [15] are also consistent with our results.

7. Conclusion

The lattice Boltzmann method presented here has been shown to provide excellent agreement with classical theoretical predictions and with lattice gas simulations. Being free from Monte Carlo noise, the computations are

[1]Note that the factor $g(\rho)$ entering the macrodynamical equations (see [5]) has been taken into account in our computation.

both fast and accurate because no averaging process is required to eliminate noise. The method is well suited to simple, rectilinear, infinite and semi-infinite boundary flows. Application to more complex geometries is possible by converting the procedure to a fully two-dimensional prescription [16,17] at the expense of loss of simplicity. However, such extensions of the method are of great interest, in particular as a next step toward the simulation of turbulence. On the other hand, microdynamical simulations can presently be conducted at reasonably high Reynolds numbers where the Boltzmann approximation is questionable. A study of the limits of validity of the Boltzmann equation method for boundary layer flows is presently in progress. As the method presented here sheds some light to the interaction mechanism between a moving fluid and a solid boundary, we are also investigating the importance of the reflection coefficient r in order to study flows subject to interactions with boundaries of variable roughness.

Acknowledgments

We acknowledge helpful discussions with D. Dab, P. Rem, and J. Somers. P.L. wishes to thank the members of the "Service de Chimie Physique" at the Université Libre de Bruxelles for their hospitality. A.N. has benefited from a P.A.I. grant. J.P.B. acknowledges support from the "Fonds national de la recherche scientifique." This work was supported by European Community Grant ST2J-0190. Part of his work was done under PAFAC Grant Z217-L128.

References

[1] J. Hardy, Y. Pomeau, and O. de Pazzis, "Time evolution of a two dimensional model system," *J. Math. Phys*, **14** (1973) 1746.

[2] J. Hardy, Y. Pomeau, and O. de Pazzis, "Molecular dynamics of a classical lattice gas," *Phys Rev*, **A14** (1976) 1949.

[3] S. Wolfram, "Statistical mechanics of cellular automata," *Rev. Mod. Phys.*, **55** (1983) 601.

[4] U. Frisch, B. Hasslacher, and Y. Pomeau, "Lattice gas automata for the Navier-Stokes equation," *Phys. Rev. Lett.*, **56** (1986) 1505.

[5] U. Frisch, D. d'Humières, B. Hasslacher, P. Lallemand, Y. Pomeau, and J.P. Rivet, "Lattice gas hydrodynamics in two and three dimensions," *Complex Systems*, **1** (1987) 648.

[6] *Discrete Kinetic Theory, Lattice Gas Dynamics and Foundations of Hydrodynamics*, R. Monaco, ed. (World Scientific, Singapore, 1989).

[7] V. Yakhot and S. Orszag, "Reynolds number scaling of cellular automaton hydrodynamics," *Phys. Rev. Lett.*, **56** (1986) 169.

[8] G.K. Batchelor, *An Introduction to Fluid Dynamics* (Cambridge University Press, Cambridge, 1967).

[9] D. d'Humières, P. Lallemand, J.P. Boon, D. Dab, and A. Noullez, "Fluid dynamics with lattice gases," in *Chaos and Complexity*, R. Livi, S. Ruffo, S. Ciliberto, and M. Buiatti, eds. (World Scientific, Singapore, 1988) 278–301.

[10] M. Knudsen, *The Kinetic Theory of Gases* (Methuen Monographs, London, 1934).

[11] D.J. Tritton, *Physical Fluid Dynamics* (van Nostrand, New York, 1977) Chapter 11.

[12] H.A. Lim, "Cellular automata simulations of simple boundary layer problems," preprint (1988).

[13] D. d'Humières and P. Lallemand, "Numerical simulations of hydrodynamics with lattice gas automata in two dimensions," *Complex Systems*, **1** (1987) 599.

[14] L.P. Kadanoff, G.R. McNamara, and G. Zanetti,"From automata to fluid flow: Comparisons of simulations and theory," *Complex Systems*, **1** (1987) 791.

[15] H.A. Lim, "Lattice gas automata of fluid dynamics for unsteady flow," *Complex Systems*, **2** (1988) 45.

[16] F.J. Higuera, "Lattice gas simulation based on the Boltzmann equation," Proc. of the workshop on *Discrete Kinetic Theory, Lattice Gas Dynamics and Foundations of Hydrodynamics*, R. Monaco, ed. (World Scientific, Singapore, 1989).

[17] S. Succi, R. Benzi, and F.J. Higuera, "Lattice gas and Boltzmann simulations of homogeneous and inhomogeneous hydrodynamics," Proc. of the workshop on *Discrete Kinetic Theory, Lattice Gas Dynamics and Foundations of Hydrodynamics*, R. Monaco, ed. (World Scientific, Singapore, 1989).